Int. J. Solids Structures Vol. 29, No. 4, pp. 399–420, 1992
Printed in Great Britain.

0020–7683/92 $5.00 + .00
Pergamon Press plc

PENETRATION OF LAMINATED KEVLAR BY PROJECTILES—I. EXPERIMENTAL INVESTIGATION

GUOQI ZHU,† WERNER GOLDSMITH and C. K. H. DHARAN
Department of Mechanical Engineering, University of California, Berkeley, CA 94720, U.S.A.

(*Received* 18 *January* 1991; *in revised form* 11 *June* 1991)

Abstract—The response of woven Kevlar/polyester laminates of varying thicknesses to quasi-static and dynamic penetration by cylindro-conical projectiles with an apex of primarily 60° has been investigated. The static properties of the material were obtained by means of standard testing procedures, including in-plane tension, compression and shear, through-thickness compression, fracture toughness and cone indentation. Compressive dynamic results were obtained using a Hopkinson bar at rates up to 2000 s^{-1}. Quasi-static force-indentation behavior for conical indenters was determined for a specimen thickness ranging from three to 10 layers to provide constitutive relations for the corresponding analytical model. These data exhibit a linear rise whose slope and peak values are proportional to specimen stiffness, followed by a plateau that terminates in a rapid reduction to a small, but finite force level when the shank of the penetrator exits. The curves were found to be highly sensitive to the size of the projectiles and the tip angle.

Static investigations were also conducted to assess the effect on penetration of specimens subject to special artificial initial conditions. This included a restraint on the global plate deformation; the use of several samples of the same total thickness, but comprised of several assemblies of stacked laminates; and embedment of an artificial delamination flaw located centrally at the midplane of the plate over approximately half of its diameter.

The dynamic tests were executed using both pneumatic and powder guns, mostly with a 12.7 mm barrel diameter. Ballistic limits were determined for these plates and terminal velocities were measured when perforation occurred. Deliberately introduced delaminations and changes in the volume fraction did not result in significant changes in the impact resistance. The damage zone created was square in shape for a 0/90 lay-up and circular for quasi-isotropic specimens. The damage pattern for dynamic loading was, however, quite different from that for the corresponding quasi-static penetration case. Kevlar laminates were found to be very resistant in arresting blunt-nosed strikers in comparison with metals on a specific weight basis.

INTRODUCTION

Laminated composites have many applications; one of the most important and widely used of these materials employs Kevlar which frequently serves as a shield in a variety of environments, such as helicopters, tanks, personnel carriers and body armor. Its primary function in these installations is the prevention of perforation of the protected surface by fragments travelling at less than ballistic speed. In consequence, an understanding of the behavior of Kevlar plates under impact conditions and, in particular, the conditions for perforation (ballistic limit) are of critical importance in the design of suitable armor.

While some information has been developed for high-speed impact, the majority of previous investigations involving impact of Kevlar and other laminated composites has focused on the low velocity regime, up to 10 m s^{-1} (ASTM, 1975; Greszczuk, 1982; Shivakumar *et al.*, 1985a, b). In this domain, it has been shown that among a variety of composites, those containing Kevlar 29 had the highest energy absorption capability (Wardle and Tokarsky, 1983; Wardle, 1982; Wardle and Zahr, 1987). Further, when a sphere is used at these speeds, the failure mechanisms of matrix cracking and delamination—with the maximum delamination shown to be linearly related to impact energy (Hong and Liu, 1989)—are of primary concern, without any consideration of fiber failure. The latter becomes critical at higher velocities when the possibility of perforation exists; few investigators have been interested in this regime. Cristescu *et al.* (1975) were concerned with the failure mechanisms of shear plugging, fiber debonding, stretching and breaking, and matrix deformation in cracking produced by the impact of a blunt projectile. Experimental investigations of matrix cracking (Takeda *et al.*, 1982a, 1987), delamination extension (Takeda

† Current address: CPC Group, General Motors Corporation, Warren, MI, U.S.A.

et al., 1982b) and wave propagation due to ballistic impact by blunt-faced cylinders (Takeda *et al.*, 1981), have been conducted. Matrix cracking in laminates struck by a sphere was studied by Joshi and Sun (1985) and by Liu and Malvern (1987).

Ballistic performance data for Kevlar have been reported by Du Pont (a, b). This information is based on standardized circular cylindrical fragments with a diameter and height of 8.75 mm and a weight of 64 grains. No data have been obtained for projectiles with conical tips. Long-rod and jet penetration of Kevlar has been studied at speeds of 1.5 km s^{-1} and the deformation mechanisms believed to have occurred in the process have been described (Scott, 1990).

The objective of the present paper is the experimental investigation of the static and dynamic penetration and perforation response due to cylindro-conical projectiles of laminated Kevlar plates. Impact speeds up to 204 m s^{-1} were employed. The quasi-static properties of the substance were determined for in-plane tension, compression and shear, through-thickness compression, fracture toughness and cone indentation. Compression Hopkinson-bar tests with strain rates up to 2000 s^{-1} were also conducted. The study required the fabrication of samples of various thicknesses, fiber orientations and volume fractions, and with various deliberately embedded flaws. The effect of multiple adjacent layers, compared to the response of a simple homogeneous target of the same total thickness, was also investigated. Material damage, resisting force, ballistic limits and terminal velocities in the penetration tests were carefully examined and, where applicable, compared to the predictions of a phenomenological model described in a companion paper (Zhu *et al.*, 1991).

SPECIMEN FABRICATION

The composites fabricated for this study consisted of woven Kevlar 29 fiber plies in a thermosetting polyester matrix. Although its modulus is lower than Kevlar 49 (used in structural composites), Kevlar 29 has superior energy absorption qualities.

Laminated plates of Kevlar 29 woven fiber (style 735) in a room temperature curing polyester matrix were manufactured by wet lay-up techniques. This is a square-weave fabric, i.e. it consists of an equal number of fibers along the two orthogonal directions woven in a 2-harness satin style, where each bundle of fibers loops alternately over and under two bundles in the orthogonal direction. The thickness of the fabric was approximately 0.61 mm, with an areal density of 491 g cm^{-2}.

The resin matrix employed was a low viscosity thermosetting polyester resin commonly used for hand lay-up at room temperature. This resin is cured at 90 C and is designed to wet easily the reinforcement fabrics employed in hand lay-up construction. The catalyst used was methyl ketone polymer (MEKP). Table 1 lists the material properties of Kevlar fiber and polyester resin.

Frabrication was conducted by first cutting 28 cm × 28 cm sections of the Kevlar sheets. Laminates were constructed with fibers in each ply oriented in the same direction (0/90) and with alternating woven plies oriented at 0° and 45° (0/90/±45, quasi-isotropic). The fabric plies were placed in a mold consisting of steel plates separated by a window frame that set the required final thickness of the laminate. The bottom steel plate, which was first coated with a release agent, was wet thoroughly with the catalyzed polyester resin before the first ply was placed on it. More catalyzed resin was applied to this first ply with a brush until it was thoroughly wet. Following this, the remaining plies were placed in the mold following the same sequence.

Table 1. Material properties of Kevlar fiber and polyester resin

	Kevlar 29	Kevlar 49	Polyester
Density (g cm^{-3})	1.44	1.44	1.12–1.46
Tensile modulus (GPa)	62	125	1.03–4.48
Tensile strength (MPa)	2758	2800–3600	28–69
Elongation to break (%)	4.0	2.4	1.7–2.6

Since the mold contained the window frame, which determined the final thickness of the laminate (and thus the final fiber volume content), there was no need to control the amount of resin placed on the fabric plies. Once all the plies were placed, the upper steel plate (also treated with release agent) was placed on top of the stack. The assembly was then inserted between the platens of a microprocessor-controlled heated platen press, a Pasadena Hydraulics model with 45 cm × 45 cm heated platens capable of a maximum compression force of 2×10^5 N. The platens were heated to 90°C and sufficient pressure was applied until the steel plates bottomed out on the window frame. The cure time was two hours to ensure complete cross-linking. The fiber volume fraction was determined to be 55% (based on weighing the fabric before impregnation, and the laminate after curing, and on using the weight density of the fiber and the resin).

The specimens with embedded delaminations were manufactured in a similar fashion except for the introduction of a circular insert of a 0.1 mm thick fluoropolymer film at the mid-plane of the laminate. All other parameters including cure temperature and fiber volume fraction were unchanged. The neat resin sample was made by mixing the resin with the catalyst and pouring the mixture into a 3.2 mm thick mold, which was then cured in an oven at 200°C.

An abrasive water jet was used to cut Kevlar 29/polyester matrix samples with clean edges, required for mechanical property experiments. For the static and dynamic penetration tests, where a clean edge was not essential, the laminated plates were cut into 14 cm diameter circular plates using a diamond band saw and then finished by abrasive grinding of the edges.

MATERIAL CHARACTERIZATION TESTS

(a) *In-plane tension and compression moduli, and Poisson's ratio measurements*

In-plane tension and compression moduli were determined by using strain gages and loading the laminate in an Instron testing machine at rates ranging from 10^{-3}–10^{-1}. Specimen dimensions were chosen for convenience as 6.3 mm (10 plies) thick and 25.4 mm wide with gage lengths of 76.2 mm and 25.4 mm for tension and compression, respectively. Poisson's ratio was found by using a strain gage at 90° to the loading direction in addition to a longitudinal strain gage. An electro-optical displacement transducer (OPTFOLLOW), described in more detail subsequently, was also used to measure the specimen elongation.

The results of the tension tests are shown in Fig. 1. The initial slope of the 0/90 laminate, about 19 GPa, decreases with further straining. This is a common observation in cross-plied laminates and is attributed to the onset of resin microcracking. Further loading results in a small increase in the modulus, possibly due to straightening of the woven fibers in the laminate. The average tangent Young's modulus over the range of loading employed in these tests was found to be 7 GPa.

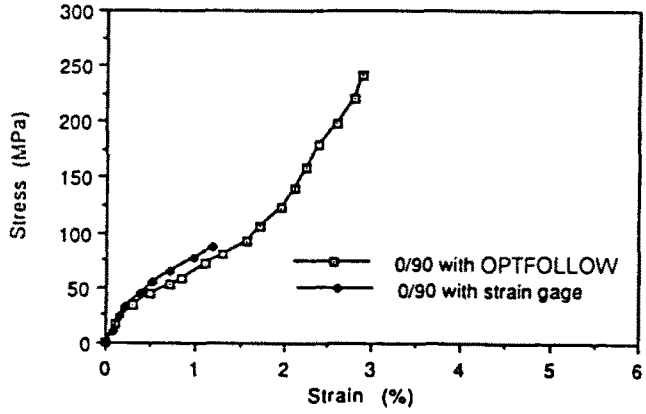

Fig. 1. Quasi-static in-plane tension test results for 0/90 laminates measured with strain gages or the OPTFOLLOW system. Specimens have a gage length of 76.2 mm and a thickness of 6.35 mm.

The rule of mixtures, which is an upper bound of the longitudinal modulus, E_1, has been found to show good agreement with measured values in continuous fiber-reinforced laminates. It is given by the expression,

$$E_1 = E_f V_f + E_m[1 - V_f] \tag{1}$$

where E_f is the longitudinal tensile modulus of the fiber, E_m is the tensile modulus of the matrix and V_f is the volume fraction of the fiber in the composite. For $V_f = 0.55$, the value of $E_f = 62$ GPa was obtained from Saghizadeh and Dharan (1986) and the value of $E_m = 1.8$ GPa was an average measurement. The longitudinal modulus E_1 is 3.49 GPa. With this value for a 0/90 weave, the laminate modulus is 17.7 GPa which is in good agreement with the measured initial slope modulus of 19 GPa. The Poisson ratio, ν_{LT} of the laminate, was measured as 0.25, using longitudinal and transverse strain gages.

The shear modulus G_{LT} can be calculated from the data resulting from tensile tests conducted on 0/90 and $\pm 45°$ laminates using the relation (Jones, 1975),

$$\frac{1}{E_{45}} = \frac{1}{4E_L} + \frac{1}{4E_T} + \frac{1}{4}\left(\frac{1}{G_{LT}} - 2\frac{\nu_{LT}}{E_L}\right). \tag{2}$$

The Young's modulus in the 45° direction, E_{45}, was measured to be 2.8 GPa. Since $E_L = E_T$ is taken as 18.5 GPa (approximately the average of the two measured values), the shear modulus G_{LT} of the laminates was determined to be 0.77 GPa. In-plane tension test data at 0/90 and at ± 45 are shown in Fig. 2.

The stress–strain curve for in-plane compression of 0/90 25.4 mm long samples using the Instron tester is shown in Fig. 3. The response is typical of a composite material in which the reinforcement phase has low compressive strength resulting in non-linear behavior. Observation of the failed specimens indicated that failure was caused by local buckling of the fibers. The poor compressive behavior and fiber buckling induced failure modes of Kevlar laminates are well known.

(b) *Through-thickness compressive strength and modulus measurements*

Through-thickness compression tests of neat polyester resin and Kevlar/polyester composites were conducted on an MTS testing system using 3.175 mm diameter, 6.35 mm thick disks, at strain rates ranging from 2.7×10^{-3} s^{-1} to 1.3×10 s^{-1}. The polyester disks were made with a core drill, while the composite disk was cut with an abrasive waterjet. The specimens were compressed by a 6.35 mm diameter punch lubricated with a Teflon coating.

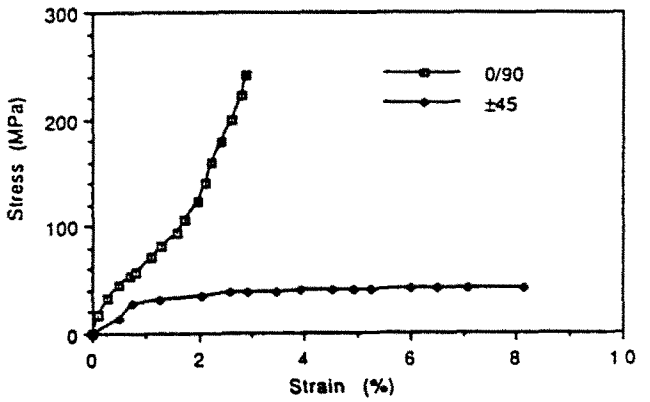

Fig. 2. Quasi-static in-plane tension data of laminates with 0/90 lay-up. Specimens have a gage length of 76.2 mm and a thickness of 6.35 mm.

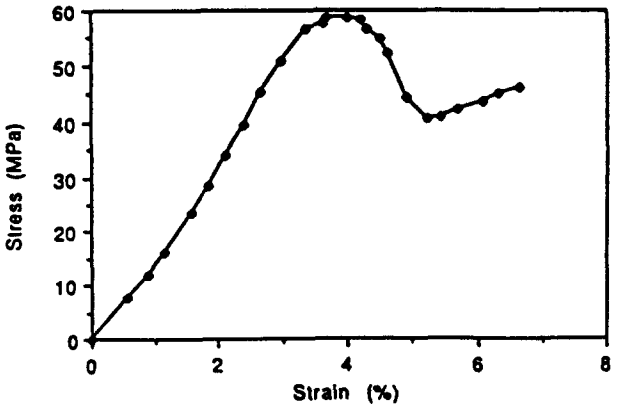

Fig. 3. Quasi-static in-plane compression results for 0/90 laminates. The specimen is 25.4 mm long and 6.35 mm thick.

The polyester resin exhibited strong rate dependence, as shown in Fig. 4. The yield stress increased 52.7% over the strain rate from 0.002 to 0.3 s^{-1}. However, the Kevlar/polyester laminates exhibited a much weaker strain rate dependence, as shown in Fig. 5, for through-thickness specimens, with only a 5.5% increase when the strain rate was changed over the

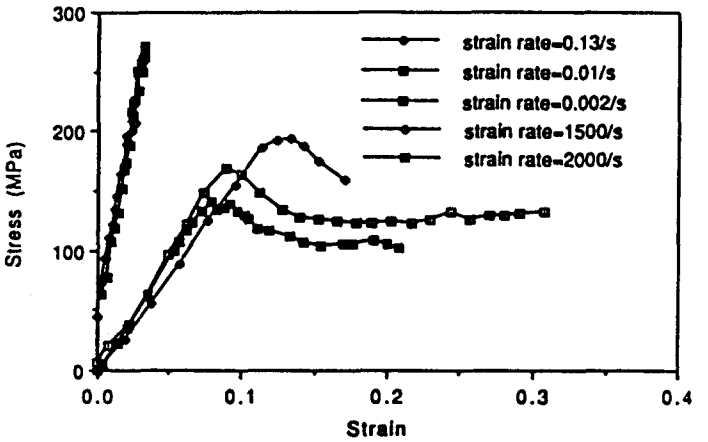

Fig. 4. Quasi-static and dynamic compression test results for polyester resin.

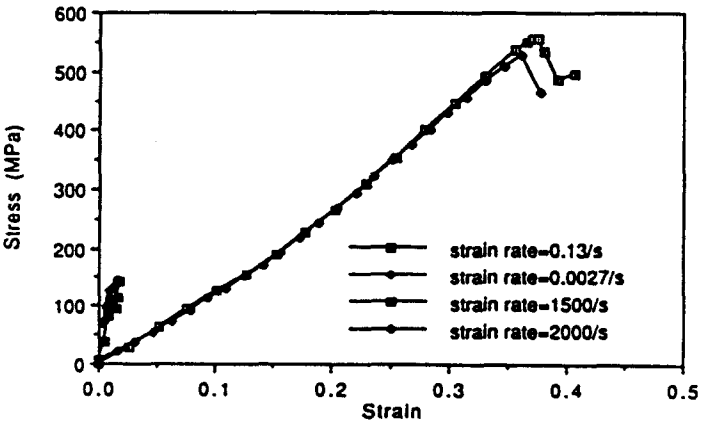

Fig. 5. Comparison of quasi-static and dynamic through-thickness compression test results for Kevlar/polyester laminates.

same range. Corresponding dynamic data from Hopkinson-bar tests at strain rates up to 2000 s^{-1} are also shown in these figures. The viscoelastic nature of both materials is evidenced by the substantially higher stresses in the dynamic response.

Data for dynamic loading of in-plane specimens is expected to exhibit a much lower rate effect as fiber behavior, which is essentially elastic, dominates specimen responses. Visual inspection of the crushed specimens of the polyester resin revealed that the material failure was due to through-thickness inward propagating radial cracks which were formed by circumferential tension. In composite specimens, the Kevlar fiber reinforcement inhibited the formation and propagation of the through-thickness cracks. Double cantilever beam specimens 25 mm wide, 3.2 mm thick, 215 mm long were used to determine the Mode I delamination using a Teflon tape generated initial mid-plane delamination 50.8 mm long. The average fracture toughness was found to be 455 ± 50 J m^{-2}; this can be compared to values of 330 J m^{-2} for Kevlar 49/epoxy and 525–1020 J m^{-2} for glass-epoxy (Saghizadeh and Dharan, 1986).

EXPERIMENTAL ARRANGEMENT AND PROCEDURE

(a) *Quasi-static tests*

Quasi-static tests on Kevlar/polyester laminates were conducted at loading rates from 10^{-3} to 10^{-1} s^{-1} to ascertain the effect of thickness, separation layers and projectile diameter on penetration characteristics and to compare observed failure phenomena with those obtained under dynamic conditions. An MTS closed-loop servo-hydraulic testing system using a load cell with a capacity of 400 kN was employed for force application. The moving crosshead could be stopped manually or by setting a voltage limit in the controller software which is run on an IBM-AT personal computer that also samples the data.

All penetrators consisted of hard-steel cylindrical projectiles with diameters of 12.7 (the standard size), 9.525 or 6.35 mm and a conical or blunt tip; cone angles employed were 60°, 90° or 120°. The various circular Kevlar specimens of 139 mm diameter were clamped in a fixture on a 114 mm diameter frame and the unit was placed on the base of the MTS machine. Plates consisted of laminates ranging from 5 to 24 layers (3.1 mm to 15 mm thick) arranged in 0/90 and 0/45 lay-ups. These included a combination of multiple plates, as well as specially prepared samples, some artificially delaminated over a portion of the surface, while others were sandwiched or backed by steel for a particular investigation. The testing machine head was lowered until the penetrator could be positioned so that its tip was just touching the center of the sample, while its flat rear surface was in contact with the head of the machine; the load was then applied. The tests were displacement controlled so that the punch could be stopped at different positions for an inspection of material damage. The load cell provided a readout of the applied force history, while displacement data were obtained from the cross head speed.

(b) *Dynamic investigation*

The dynamic penetration tests utilized 12.7 mm and 9.5 mm diameter cylindro-conical oil-hardened steel projectiles (62 R_c) with a 60° tip angle, lengths of 38.1 and 34 mm and masses of 28.9 and 15.4 g, respectively, to determine the ballistic limits of various Kevlar composite combinations or the terminal velocity when complete perforation occurred. A single test utilizing a flat-nosed striker was conducted to portray the difference in target response between a blunt and a sharp-nosed projectile.

The propulsion equipment consisted of a pneumatic and two powder guns, all mounted on a heavy steel table located in an isolation chamber requiring remote firing. The pneumatic gun featured a barrel with an inside diameter of 12.7 mm and a length of 1.3 m mounted on its support by three brackets. A solenoid valve separated the breech from a reservoir containing nitrogen stored at the desired pressure by means of a control valve. A maximum pressure of 102 atm can be achieved, transmitted from the supply cylinder which is charged to 153 atm. Solenoid activation provides access of the back pressure to the rear of the projectile and initiates the launch.

Two separate powder guns with barrel diameters of 12.7 and 9.5 mm, respectively, were connected to the table at the breech by a massive brace. Projectiles for these impact-activated devices were coated with copper to minimize barrel wear. The breech of the former can accommodate 20 mm shells, but a 50 caliber shell was used for most of the tests fired at velocities of about 300 m s^{-1} and for the single shot conducted with this diameter that was propelled at 800 m s^{-1}. The smallest-sized gun was adapted from a commercial Magnum; its breech houses shells that are specifically designed for its bullet size. Rounds were assembled individually: a steel shell with a volume of 6.48 cc filled with Du Pont IMR 3031 black powder, reusable upon replacement of the primer, was inserted into the breech just behind the 12.7 mm diameter projectile placed in the barrel. The maximum speed obtainable with the steel shell is 1000 m s^{-1}; substantially higher velocities can be achieved by use of a brass shell which can accommodate more powder. The 9.52 mm diameter striker was inserted into the tip of the corresponding brass shell that was then loaded into the Magnum breech; these shells were used repeatedly upon replacement of the primer.

Most of the targets were made of Kevlar laminates with a 45% matrix volume fraction; a few consisted of smaller matrix volume fractions of 35% and 26%. The majority of the targets were fully clamped on a 114.3 mm diameter target holder which was also mounted on the steel table. A few samples were constrained only over a portion of the periphery to permit photographic observation of the penetration process. All specimens were located normal to the projectile trajectory which intersected the target at its center.

The initial velocity of the pneumatically-propelled projectile is measured from the interruption upon bullet passage of two lasers focused onto two photodiodes, 152 mm apart, passing through two slots in the barrel on opposite sides of a diameter. These slots also serve to vent the back pressure and thus prevent further acceleration of the striker. The change in voltage due to beam extinction is recorded on a Nicolet digital oscilloscope. In the case of the powder gun, the laser beams are located just ahead of the gun muzzle.

A Beckman-Whitley model WB-2 high speed camera featuring a motor driven rotating prism, with framing rates ranging from 20,000 to 10^6 frames s^{-1}, was employed to observe the motion of the projectile and target during penetration. There are 79 separate lens stages and corresponding light paths focused onto the stationary Kodak Tri-X (400 ASA) 35 mm film. The motor speed is controlled by a rheostat and continuously displayed on a time-interval meter from a signal emitted upon passage of a protrusion on the rotor by a stationary magnet. The light source was a stroboscopic unit with a single flash capability of sufficient duration to illuminate the process for the duration of a quarter-circle sweep of the prism, about 1.8 ms. It was activated by a signal obtained from the interruption of the second laser beam delayed by a device so that the flash duration corresponded to the impact event.

The final projectile velocity is obtained by means of two aluminum screens spaced 235 mm apart, located just behind the target. Each screen is composed of two aluminum foils taped on the surface of a 10 mm thick wooden frame. One foil is directly connected to an oscilloscope, while the second foil of each set is connected serially to a 6 V battery and then to the oscilloscope. This unit is not subjected to a voltage initially, since the foils are separated. When the projectile perforates each of the two screens, two foils are connected by the conductive projectile, and two signals are thus imposed on the recorder, permitting the calculation of the terminal striker speed.

An OPTFOLLOW 7000C electro-optical displacement system† was used to track the motion of the projectile. This unit consists of a camera and a microprocessor control and monitors the movement of the interface between a black and white region with a digital output transmitted to an oscilloscope. The device is calibrated quasi-statically by moving such a boundary in the plane orthogonal to the camera at the same distance as used in the dynamic test to achieve the proper field of view. In the dynamic application, the camera follows the tail of the projectile on which the boundary is marked, its path being uniformly illuminated by two DC lights. A background with a black and white boundary is placed on the opposite side of the projectile path from the camera. When focused on the path of the

† Yaman Ltd., San Jose, CA, U.S.A.

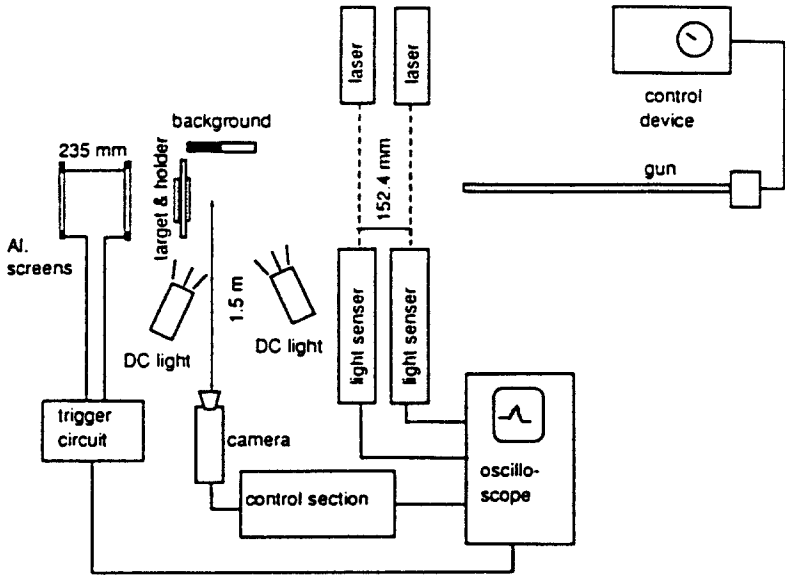

Fig. 6. Schematic of experimental arrangement using the OPTFOLLOW system.

projectile, the OPTFOLLOW recognizes the blurry boundary on the background before the projectile appears in the field of view. The clear boundary on the projectile overlaps the blurry boundary when the projectile enters the view of the OPTFOLLOW. The unit now switches to track the motion of the boundary on the projectile, resulting in an electrical signal. The framing camera and the OPTFOLLOW unit could not be used concurrently.

All operations were performed from outside the chamber. The signal produced by the interruption of the first laser beam was fed into a Tektronix AM502 differential amplifier and sequentially to a delay unit whose output was employed to trigger the stroboscope. The proper delay time was calculated from the anticipated projectile speed and the distance from the first laser to the target.

Operation of the OPTFOLLOW system required proper setting of the control unit, the establishment of a suitable field of view and a subsequent initial calibration; two methods were used for the latter procedure. In the first, a dummy projectile was slowly moved through the viewing window so that the output could be correlated with the position of the projectile. The second method involved the firing of the striker through this region at constant velocity, whose value was obtained from laser measurements. This provided a calibration factor for the concurrent OPTFOLLOW output. A schematic of the experimental arrangement for the OPTFOLLOW system is shown in Fig. 6.

RESULTS AND DISCUSSION

(a) *Static tests*

The load–displacement curves of Kevlar/polyester laminates ranging from 5 to 10 plies perforated quasi-statically by a 60° conically-nosed steel penetrator are presented in Fig. 7; these combine the local indentation and the global deflection of the plate. Both the initial slope, which is a measure of the global deflection, and the maximum resistance of the laminates increased with thickness. The first peak on the curves corresponds to the initiation of fiber failure which occurred on the distal side and is due to local bending and bulging of the material. An increase in the laminate thickness reduces global deflection for a given load and delays fiber failure. The thinner plates exhibit a load plateau with small oscillations occasioned by continuing fiber failure; for the thicker specimens, the load in this plateau domain relaxes at an increasing rate as the number of layers increases. This is attributed to the breakage of a larger number of fibers after initial penetration than occurs for laminates containing a smaller number of plies.

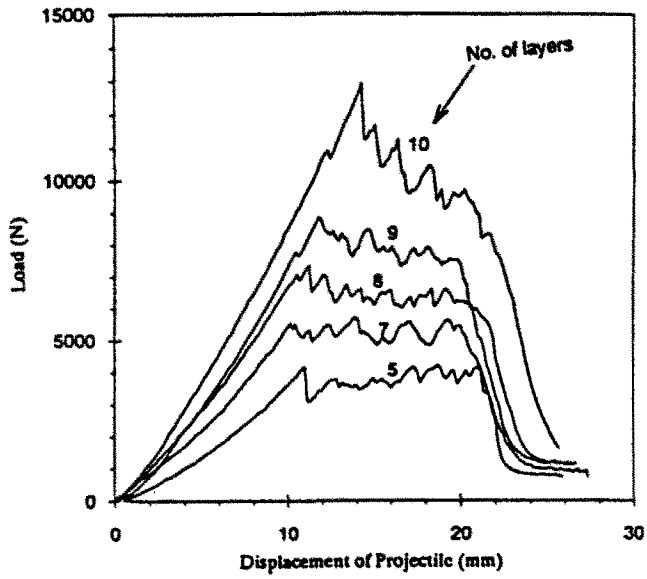

Fig. 7. Load-displacement curves of the quasi-static perforation of Kevlar/polyester laminates with thicknesses ranging from 5 to 10 plies by a 12.7 mm diameter hard steel cylinder with a 60° tip angle. The loading speed is 12 mm min^{-1}.

Figure 8 presents four sectioned samples at successive stages of quasi-static loading to a 10-ply (6.35 mm thick) laminate by a 12.7 mm diameter cylindro-conical steel projectile with a 60° tip angle, corresponding to an advance of the projectile in increments of 6.35 mm. These photographs depict three of the four most important responses of the plate when it is subjected to increasing load by a sharp-tipped penetrator; this behavior is characteristic of specimens of moderate thickness. Initially, Fig. 8a, only global plate deflection is observed. In the next stage, Fig. 8b, some fiber failure and bulging at the distal side is manifested. The next two phases show an increasing pattern of fiber failure until complete perforation occurs; this process is accompanied by a successively reduced global deformation. In addition, delamination is present which cannot be distinguished in the photographs. The dominance of the global deformation process does not have a counterpart in the dynamic case because the energy of deformation is transformed into that of traveling waves and the system is not in a state of equilibrium.

The effect of a restraint on global deformation is shown in Fig. 9 where two 10-ply laminates, clamped around the edges, but unrestrained in back or supported by an adjacent steel plate with a 25.4 mm central hole, respectively, were perforated by a 12.7 mm cylindro-conical steel projectile with a 60° tip. The peak load for the two cases is about the same, but the restrained system exhibits a much lower deflection both at the maximum load and at complete perforation. Thus, the energy consumed in global deformation of the backed plate is about 60% of that of the unrestrained case where it represents a significant fraction of the total consumed during the perforation process.

The quasi-static perforation of several laminates with a total of 24 plies was also investigated to assess the performance of a homogeneous target relative to that composed of several plies of the same total thickness. The samples consisted of a single 24-ply laminate as well as adjacent blocks of 2×12, 3×8 and 4×6-ply laminates; the test results are shown in Fig. 10. The bending stiffness of the targets decreased with the increasing number of adjacent, but unconnected layers. At the initiation of perforation, up to which point global deformation constitutes the major energy absorption mechanism, the four-ply sample absorbed approximately 68% of the energy of the homogeneous laminate and exhibited 58% of its peak load. These figures provide an idea of the effect of delamination; however, these values differ substantially from those for the case of pure bending. The reasons for this discrepancy are largely due to the presence of a sharp tip and the transfer of loading in the tests from pure bending to in-plane tension.

The quasi-static loading curve for a 10-ply laminate with an embedded delamination of 85 mm diameter and that of a fully laminated plate when perforated by a 12.7 mm diameter, 60° cylindro-conical steel projectile are presented in Fig. 11. The loading pattern was transformed from bending to in-plane tension. The delaminated specimen has a lower initial slope and a slightly lower peak load, corresponding to the initiation of effective fiber failure, that occurs at a significantly greater displacement. However, the energy absorbed in view of the more rapid unloading for this case is approximately 10% lower than for the intact specimen. Both of these results are qualitatively confirmed by the data shown in Fig. 10.

The size of the penetrator also plays a key role in the response of the composite to quasi-static loading. Experiments were conducted using 12.7, 6.35 and 3.175 mm steel cylinders with 60° conical tips to perforate both 20- and 10-ply laminates; the results are shown in Fig. 12. The initial slope for these three cases is about the same, but the peak force is roughly proportional to the diameter of the projectile. A comparison of the response of the 10-ply laminate with that of the 20-ply sample upon loading by the same (12.7 mm) penetrator indicates the divergence in the slope, previously noted, and a peak force ratio of one-half, with unloading occurring sooner for the thinner plate.

The effect of the cone angle of a 12.7 mm penetrator on the response of a 10-ply sample is presented in Fig. 13. The initial slopes for the 60°, 90° and 120° tips are almost the same because global deflections dominate at this stage. The peak force increased with tip angle, as expected, amounting to a 40% difference over the range investigated with a corresponding increase in the energy absorbed by the plate. Figure 14 shows the distal side of the sample upon perforation by the 120° tip projectile, together with the plug produced. This was the only instance of plugging found in the present investigation. This type of phenomenon is similar to that observed in metallic targets and some other composites when a blunt projectile strikes at a speed above the ballistic limit. In contrast, a blunt projectile did not perforate a 10-ply laminate under quasi-static conditions; the large forces applied resulted in the specimen being pulled out of the clamp with severe distortion and delamination.

(c) *Dynamic investigations*

The ballistic limits of Kevlar laminates with random fiber orientations as a function of their thickness, a structural property of the system, were determined for both 9.525 and 12.7 mm diameter 60° cylindro-conical steel projectiles with masses of 12.5 and 28.9 g, respectively. This limit was considered here to have been attained when the projectile was either stuck in the target as shown in Fig. 15, or else exited with negligible velocity. The difference in these conditions is considered to be a variation in initial speed of less than 5 m s^{-1}. The results are shown in Fig. 16; within this range, the ballistic limit varies linearly with laminate thickness and is higher for the smaller striker due to its lower mass. A similar conclusion was reached by Bless *et al.* (1985) for glass composites penetrated by a hemispherically-nosed projectile. The smaller projectile exhibits a slightly steeper slope. The ballistic limit of 3.175 mm thick 2024-0 aluminum plates struck by the 12.7 mm diameter cylindro-conical projectile was about 90 m s^{-1} (Bless and Hartman, 1989); on the basis of areal density, the Kevlar has an equivalent ballistic limit of 110 m s^{-1}, 20% greater than that for aluminum.

Laminates with various lay-ups as well as with an embedded delamination between two layers of 40 mm diameter were examined to assess the effects of these factors on dynamic perforation. The results, indicated in Fig. 17, show the final velocity of the projectile as a function of the initial speed and indicate that neither lay-up nor prior partial delamination played a significant role in the perforation phenomenon.

On the other hand, Fig. 11 indicates that the effect of a delamination was a reduction of 10% in the energy absorption during quasi-static loading. The ballistic limit for a 5-ply Kevlar plate with a single-level 40 mm diameter delamination was found to be 13% less than that of a full-strength sample. As the impact speed increases above the ballistic limit, this difference rapidly disappears, and partly delaminated specimens exhibit the same resistance as intact samples. As in similar cases of comparison of theory and experiment

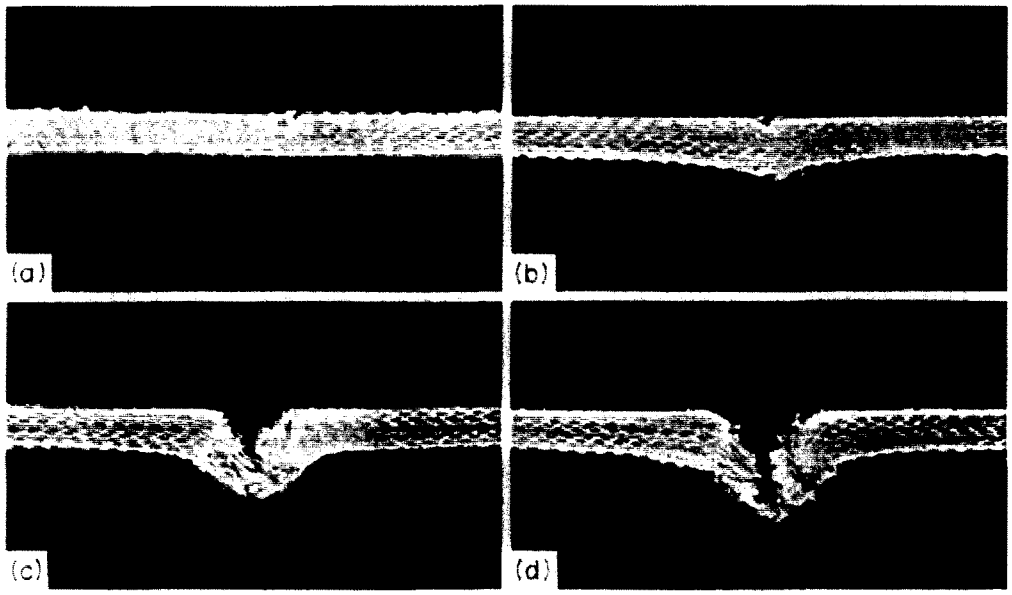

Fig. 8. Photographs of the damage in four 6.35 mm Kevlar/polyester laminates due to quasi-static penetration by a 12.7 mm diameter hard steel cylinder with a 60° tip angle to various end positions from a fixed reference: (a) 6.35 mm, (b) 12.7 mm, (c) 19.05 mm and (d) 25.4 mm. The loading speed is 12 mm min^{-1}.

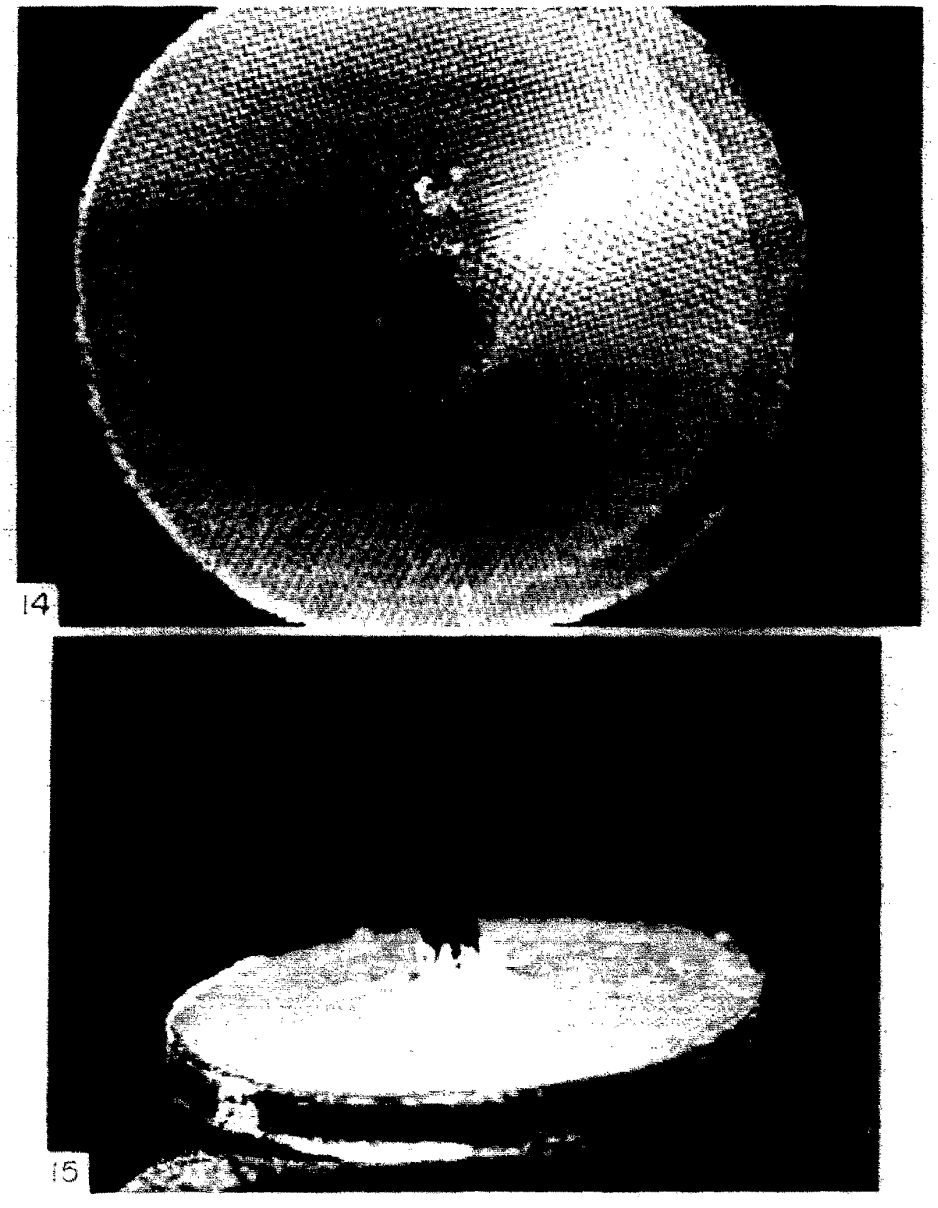

Fig. 14. Damage due to the 120° penetrator whose action is shown in Fig. 12. A plug was generated.

Fig. 15. Photograph of a 20-ply target perforated by a 12.7 mm diameter, 60° cylindro-conical projectile of 32.2 g mass at the ballistic limit (initial velocity = 170 m s^{-1}).

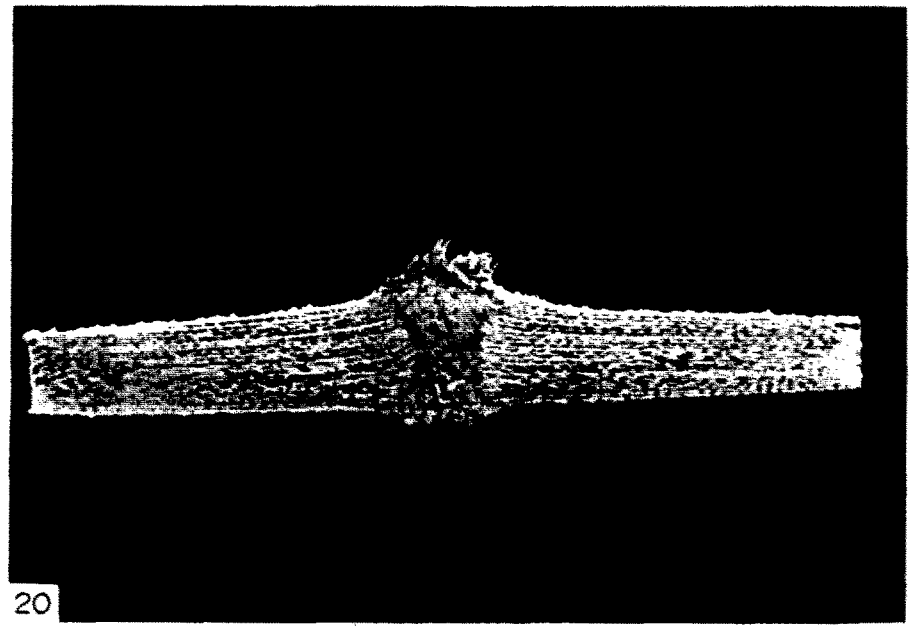

Fig. 19. Exit side damage in a 10-ply laminate due to perforation by a 60°, 12.7 mm diameter projectile at an initial velocity of 783 m s^{-1}.

Fig. 20. Cross-sections of a 20-ply laminate perforated by a 60°, 12.7 mm diameter cylindro-conical projectile at an initial velocity of 236.5 m s^{-1}.

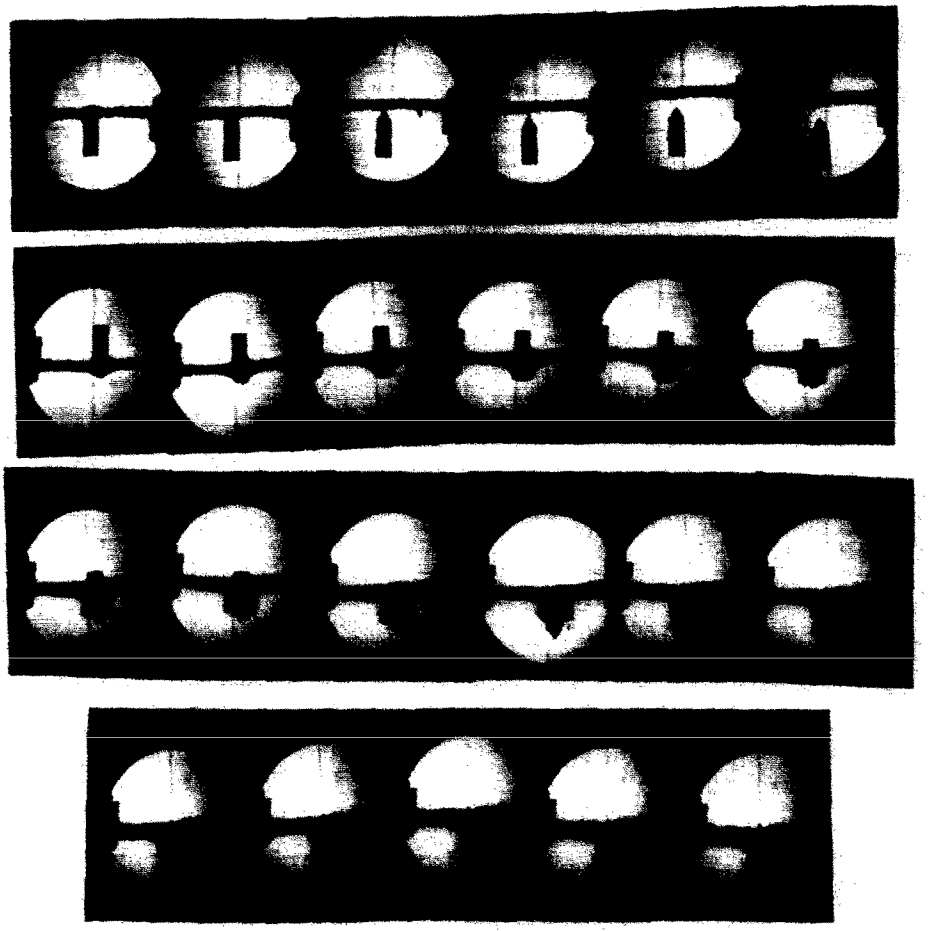

Fig. 21. High-speed photographs of a 10-ply laminate perforated by a 60°, 12.7 mm diameter cylindro-conical projectile at an initial velocity of 188.6 m s^{-1}. The framing rate is 20.2 μs/frame.

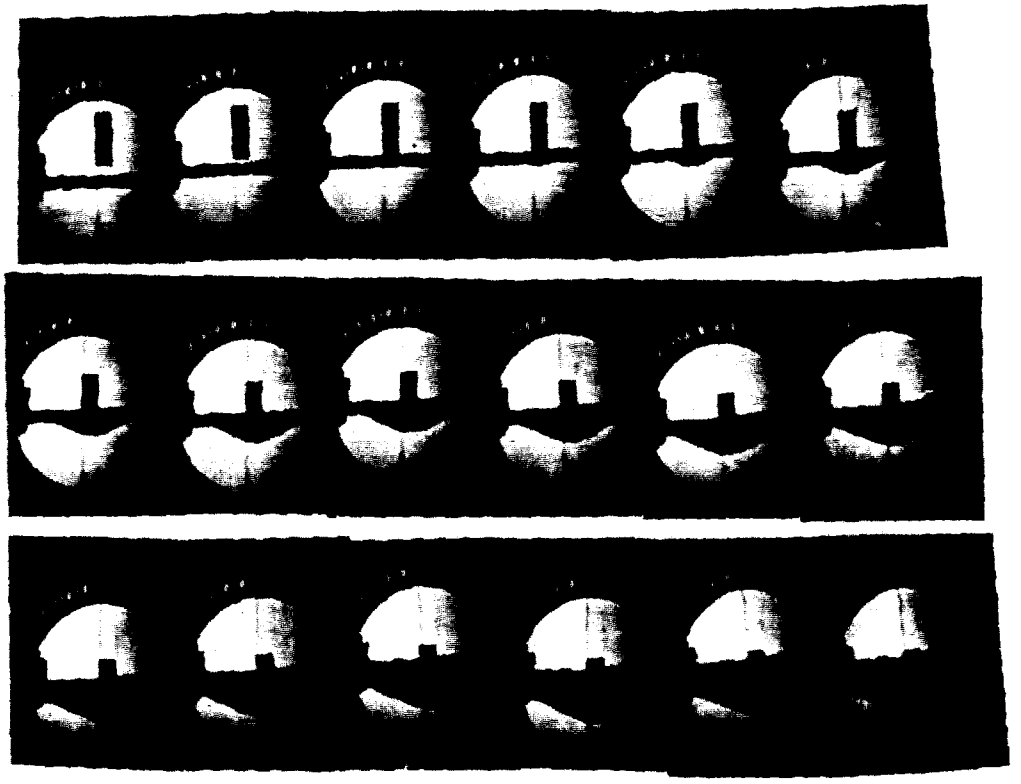

Fig. 22. High-speed photographs of a 10-ply laminate struck by a 12.7 mm diameter blunt hard-steel projectile at an initial velocity of 170 m s^{-1}. The framing rate is 20.2 μs/frame.

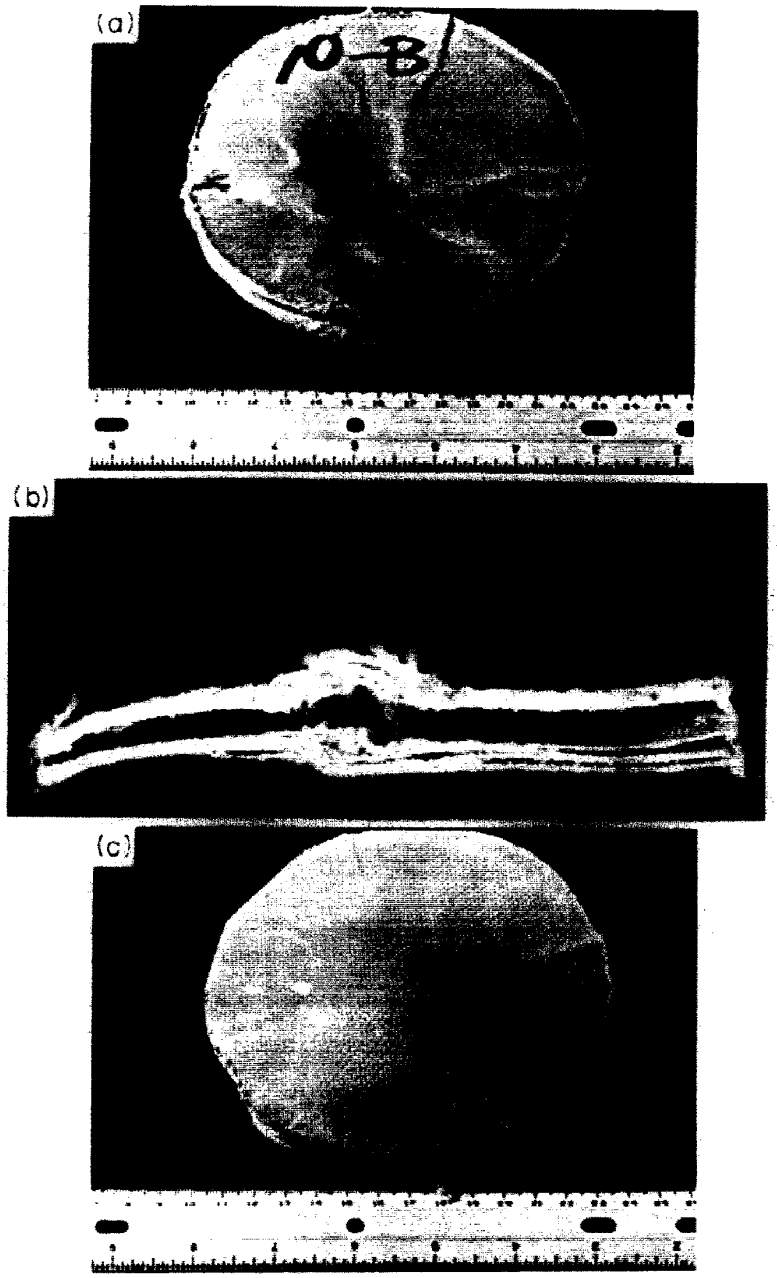

Fig. 23. Damage to the specimen shown in Fig. 22: (a) Impact side; (b) Cross-section; (c) Distal side.

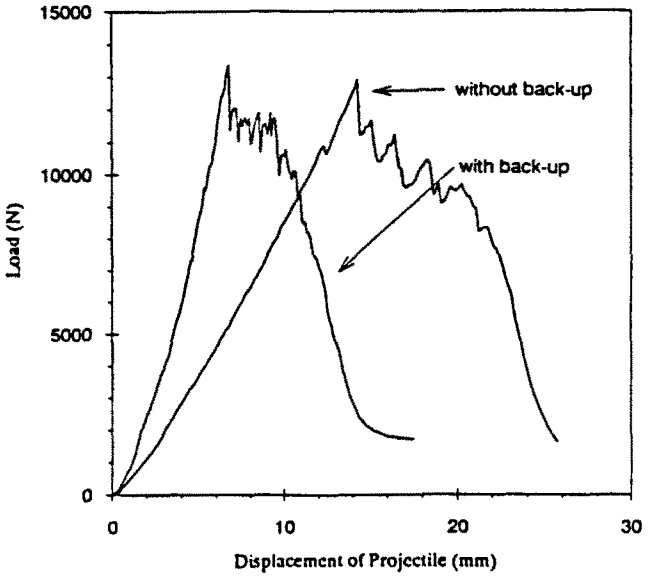

Fig. 9. Load–displacement curves of the quasi-static perforation by a 12.7 mm diameter cylindro-conical penetrator of a 6.35 mm thick laminate with and without a back-up of a steel plate with a 5.4 mm diameter central hole.

involving metals (Landkof and Goldsmith, 1985), a discrepancy near the ballistic limit is more likely to occur because of the importance of certain mechanisms (neglected in an analysis) whose effect becomes negligible when the initial striker speed is well above the critical value. Sectioned specimens examined visually exhibited a delamination radius of 25–45 mm diameter, well below those used in the artificially separated targets; the exact extent of the cracks was difficult to measure because the dye penetrant did not clearly delineate the fracture region. This confirms the finding that the global deformation absorbs proportionally a much lower amount of energy in the higher velocity regime, unlike the situation under quasi-static loading.

Similarly, the effect of varying the volume fraction of the matrix in a 5-ply laminate was investigated relative to the dynamic resistance. As shown in Fig. 18, the terminal velocity and the ballistic limit vary only between 75 and 77.9 m s^{-1}, and are not affected, within experimental error, by changes in composition over the range of V_m = 26% to 45% examined here. This compares to the 10% difference in ballistic limits for Kevlar/polymer combinations involving various volume fractions perforated by cylindrical bullets of 8.75 mm diameter and a mass of 4.15 g (Du Pont (b)).

The distal side view of a 10-ply laminate due to very high-speed perforation (initial velocity v_0 = 783 m s^{-1}) by a 60°, 12.7 mm diameter bullet is presented in Fig. 19. The principal damage is clearly fiber failure; a substantial bundle has been detached from the matrix and pushed along the direction of the striker motion. The shape of the damage region depends upon the weave and lay-up of the target. A 0/90 laminate showed a square-shaped damage zone on the distal side with an extent 1.5–2 times the projectile diameter, similar to the static case. A random lay-up resulted in a circular pattern. As only one type of weave was utilized in the present tests, the effect of weave geometry could not be determined. It was reported (Du Pont (b)), that while fabrics with smaller size yarns were superior to constructions based on larger size yarns in resisting perforation of handgun projectiles, neither yarn size nor weave pattern seemed to affect the penetrability of fragments.

The delamination in perforated plates was studied by noting the damage in sections of the target. This region was generally found to be 25–45 mm in length, as shown in Fig. 20. Bulging and fiber failure are also depicted in this photograph.

The perforation process was captured by high-speed photography, as shown in Fig. 21 for a 10-ply laminate struck by a 60°, 12.7 mm diameter bullet at a velocity of

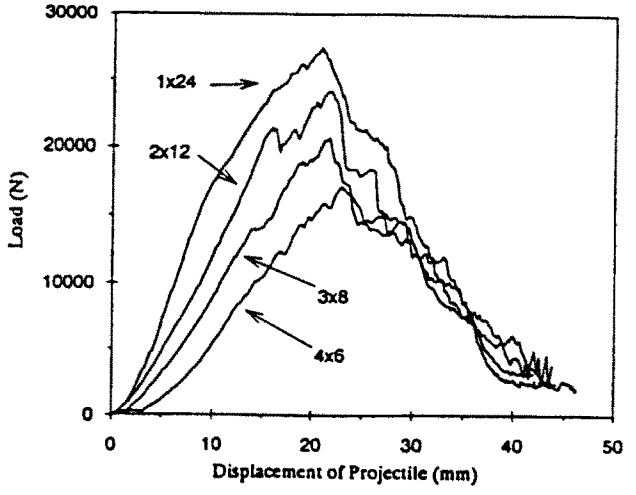

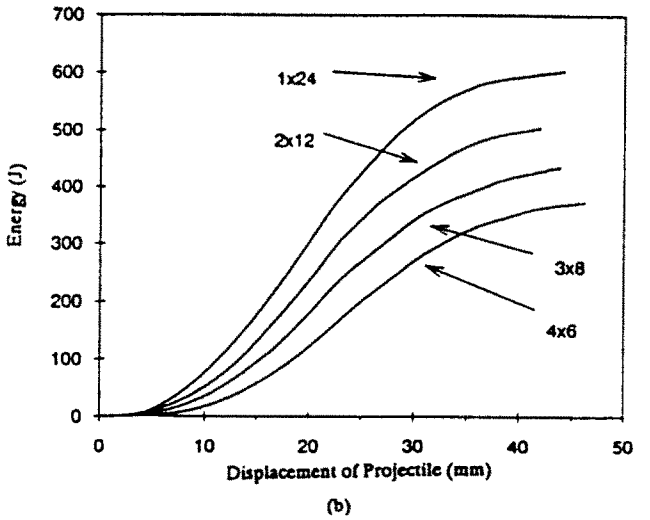

Fig. 10. Load–displacement (a) and energy–displacement curves (b) for the quasi-static perforation by a 12.7 mm diameter penetrator with a 60° tip angle of various adjacent layered Kevlar/polyester targets with a total thickness corresponding to 24 plies. Loading speed is 12 mm min^{-1}.

188.6 m s^{-1}. The framing interval was 20.2 μs. This sequence depicts the evolution of the event, with initial bulging and subsequent dominant fiber failure, but relatively small global deformation due to an initial speed approximately 50% above the ballistic limit.

A similar test using a blunt projectile striking a 10-ply target at a speed of 170 m s^{-1} is depicted in Fig. 22. The sequence exhibits the enormously greater global displacement of the plate and correspondingly large delaminations, but the absence of any significant penetration; the deformed impact and distal sides of the specimen as well as a central section are presented in Fig. 23. The large global deformations are clearly evident; the laminate was found to be wrinkled with delaminations extending to the outer border. A plug with the diameter of the projectile had been sheared out of only the first layer (0.635 mm thick). Clearly, the material exhibits a much better perforation resistance to blunt projectiles compared to sharp-nosed strikers.

An analytical model of the dynamic perforation process has been developed which takes into account global plate deformation, bulging on the distal side, penetration of the conical striker, delamination and fiber failure. This work, as well as a comparison of its predictions with experimental data, is presented in a companion paper (Zhu *et al.*, 1991).

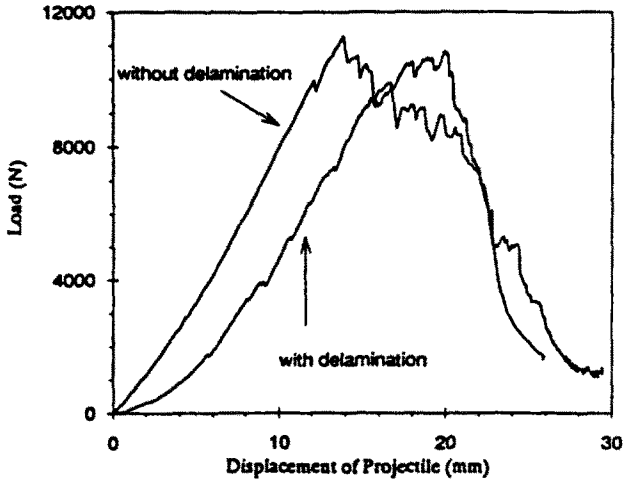

Fig. 11. Load–displacement curves of the quasi-static perforation of 10-ply laminates with and without a built-in 85 mm radius central delamination by a 12.7 mm diameter penetrator with a 60° conical tip. Loading speed is 12 mm min^{-1}.

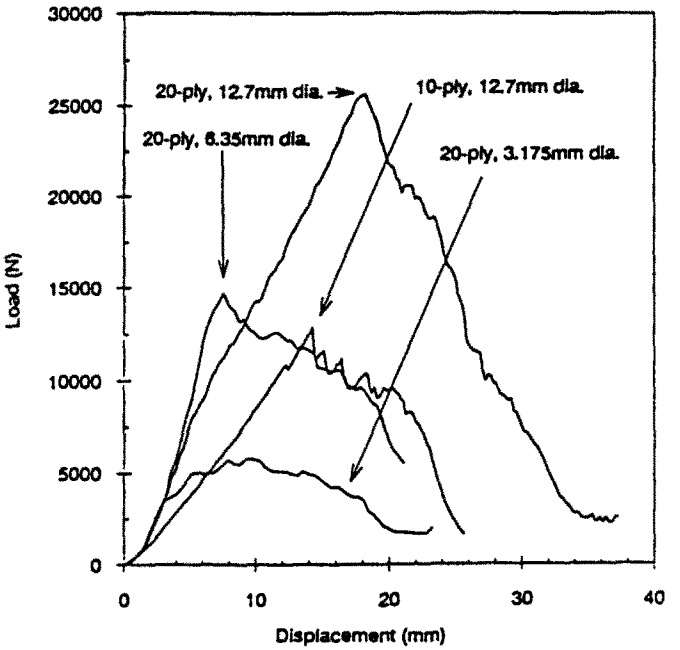

Fig. 12. Load–displacement curves of the quasi-static perforation by 60° cylindro-conical hard steel penetrators with diameters of 3.75, 6.35 and 12.7 mm.

CONCLUSIONS

An experimental investigation of the static and dynamic penetration of various Kevlar/polyester laminates primarily by sharp-pointed projectiles has been conducted for various laminate constructions, target thicknesses and impact speeds. The hard-steel strikers were generally cylindro-conical with a tip angle of 60°; a 12.7 mm diameter projectile had a mass of 28.5 g, while the 9.525 mm diameter striker had a mass of 12.5 g. It is concluded that:

(1) Global and shear stiffness played a very important role in resisting quasi-static penetration, but were of considerably smaller importance in dynamic tests.

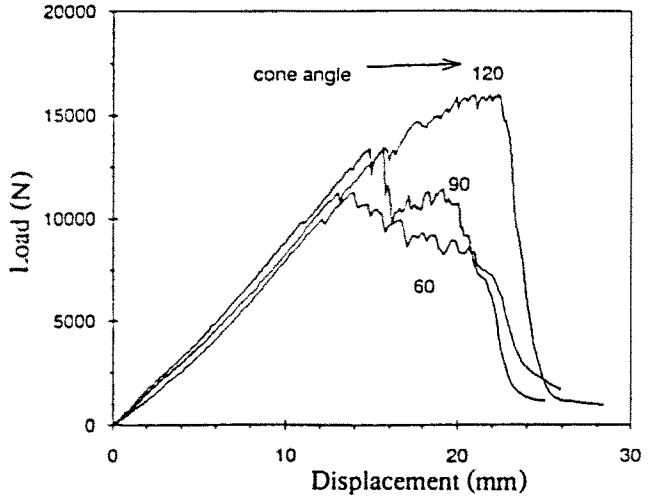

Fig. 13. Load–displacement curves of the quasi-static perforation of 10-ply laminates by 12.7 mm diameter cylinders with cone angles of 60°, 90° and 120°.

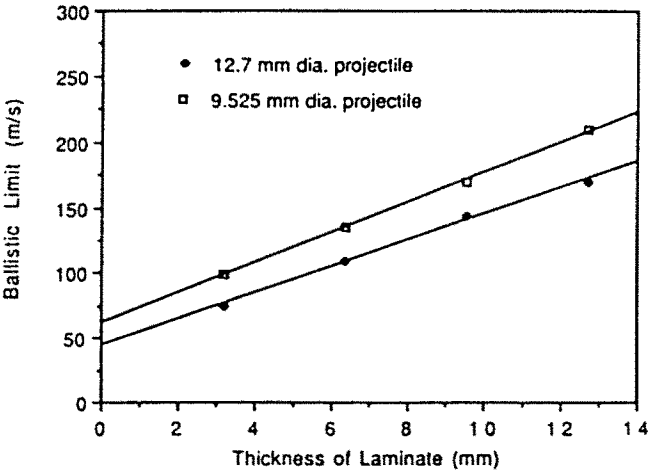

Fig. 16. Ballistic limits of Kevlar/polyester composites penetrated by 60° cylindro-conical projectiles with two different diameters.

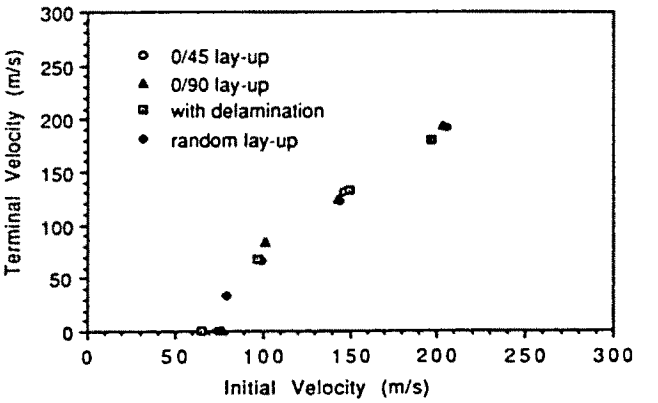

Fig. 17. Terminal velocity as a function of initial striker speed for the perforation of 5-ply laminates of various constructions by a 60°, 12.7 mm diameter cylindro-conical projectile.

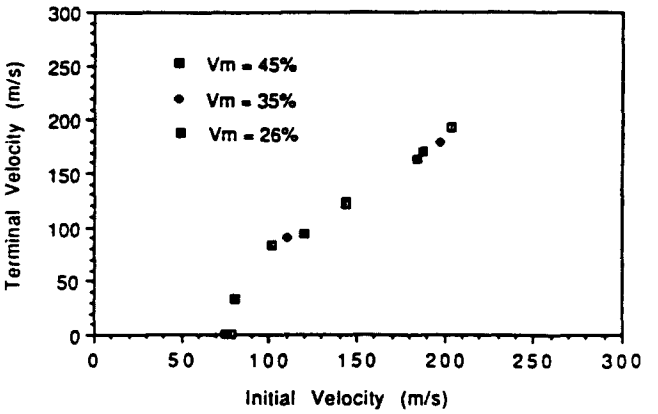

Fig. 18. Effect of matrix volume fraction on the ballistic performance of a 60 , 12.7 mm diameter projectile striking a 5-ply target.

(2) Local deformation and fiber failure constituted the major energy absorption mechanisms in impact perforation. This is documented both by high speed photography and by post mortem examination of the targets.

(3) The existence of deliberately introduced delaminations, changes in the fiber volume fraction and variations in the lay-up did not significantly influence impact resistance, but affected static penetration to a greater degree. Delamination, either in the static or dynamic case, did not seem to dissipate a major amount of energy.

(4) Perforation with blunt 12.7 mm diameter steel projectiles could not be achieved in 10-ply laminates in the velocity range up to 200 m s^{-1} compared to a ballistic limit of 75 m s^{-1} for cylindro-conical strikers.

(5) Kevlar laminates exhibit better impact resistance to cylindro-conical projectiles on a specific weight basis when compared to aluminum.

REFERENCES

ASTM STP 568 (1975). *Foreign Object Impact Damage to Composites*. ASTM, Philadelphia.

Bless, S. J., Hartman, D. R. and Hanchak, S. J. (1985). *Ballistic Performance of S-2 Glass Laminates*. Univ. of Dayton Research Institute, UDR-TR-85-88A.

Bless, S. J. and Hartman, D. R. (1989). Ballistic penetration of S-2 glass laminates. *Proc. 21st SAMPE Conf.* (Edited by R. Wegman *et al.*), pp. 852–866.

Cristescu, N., Malvern, L. E. and Sierakowski, R. L. (1975). Failure mechanisms in composite plates impacted by blunt-ended penetrators. In ASTM STP 568, 159–172.

Du Pont Corporation (a). Kevlar lightweight protective armor. Wilmington, DE Publication E-60153.

Du Pont Corporation (b). Composite armor technical information. A guide to designing and preparing ballistic protection of Kevlar aramid, Publication E-09164.

Greszczuk, L. B. (1982). Damage in composite materials due to low velocity impact. In *Impact Dynamics* (Edited by L. A. Zukas *et al.*), pp. 55–94. John Wiley & Sons, New York.

Hong, S. and Liu, D. (1989). On the relation between impact energy and delamination area. *Exp. Mech.* **29**, 115–120.

Jones, R. M. (1975). *Mechanics of Composite Materials*. McGraw-Hill, New York.

Joshi, S. P. and Sun, C. T. (1985). Impact induced fracture in a laminated composite. *J. Comp. Mater.* **19**, 51–66.

Landkof, B. and Goldsmith, W. (1985). Petaling of thin, metallic plates during penetration by cylindro-conical projectiles. *Int. J. Solids Structures* **21**, 245–266.

Liu, D. and Malvern, L. E. (1987). Matrix cracking in impacted glass/epoxy plates. *J. Comp. Mater.* **21**, 594–609.

Saghizadeh, H. and Dharan, C. K. H. (1986). Delamination fracture toughness of graphite and aramid epoxy composites. *J. Engng Mater. Tech.* **108**, 125–130.

Scott, B. R. (1990). The penetration of Kevlar laminate by long rods and jets. *Proc. 12th International Symposium on Ballistics* **3**, 42–49.

Shivakumar, K. N., Elber, W. and Illg, W. (1985a). Prediction of impact force and duration due to low-velocity impact on circular composite laminates. *J. Appl. Mech.* **52**, 674–680.

Shivakumar, K. N., Elber, W. and Illg, W. (1985b). Prediction of low-velocity impact damage in thin circular laminates. *AIAA Jl* **23**, 442–449.

Takeda, N., Sierakowski, R. L. and Malvern, L. E. (1981). Wave propagation experiments on ballistically impacted composite laminates. *J. Comp. Mater.* **15**, 157–174.

Takeda, N., Sierakowski, R. L. and Malvern, L. E. (1982a). Microscopic observation of cross sections of impacted composite laminates. *Comp. Tech. Rev.* **4**, 4–10.

Takeda, N., Sierakowski, R. L., Ross, C. A. and Malvern, L. E. (1982b). Delamination-crack propagation in ballistically impacted glass/epoxy composite laminates. *Experimental Mech.* **22**, 19–25.

Takeda, N., Sierakowski, R. L. and Malvern, L. E. (1987). Transverse cracks in glass/epoxy cross-ply laminates impacted by projectiles. *J. Materials* **19**, 51–66.

Wardle, M. W. (1982). Impact damage tolerance of composites reinforced with Kevlar aramid fibers. *Prog. Sci. Engng Comp.* Proc. ICCM-IV in Tokyo.

Wardle, M. W. and Tokarsky, E. W. (1983). Drop weight impact testing of laminates reinforced with Kevlar aramid fibers, E-glass and graphite. *Comp. Tech. Rev.* **5**, 4–10.

Wardle, M. W. and Zhar, G. E. (1987). Instrumented impact testing of aramid-reinforced composite materials. ASTM STP 936, 219–235.

Zhu, G., Goldsmith, W. and Dharan, C. K. H. (1991). Penetration of laminated Kevlar by projectiles—II. Analytical model. *Int. J. Solids Structures* **29**, 421–436.